Cell Reports
Medicine

Report

Neutralizing-antibody-independent SARS-CoV-2 control correlated with intranasal-vaccine-induced CD8$^+$ T cell responses

Graphical abstract

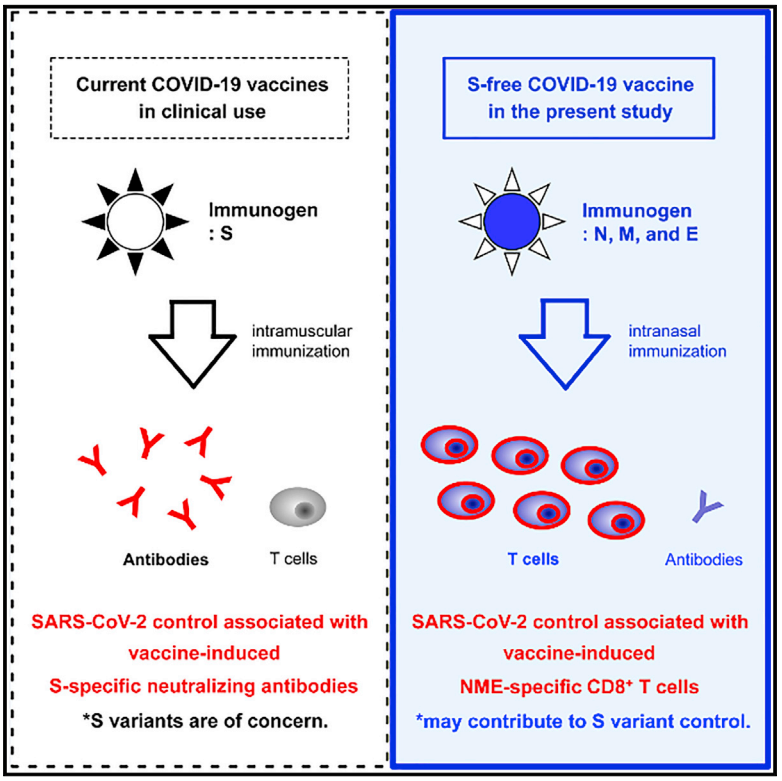

Highlights

- Anti-SARS-CoV-2 efficacy of an intranasal S-free vaccine is shown in macaques
- The SARS-CoV-2 control is associated with vaccine-induced CD8$^+$ T cell responses
- Vaccine induction of CD8$^+$ T cells can result in neutralization-free viral control
- Vaccine-induced CD8$^+$ T cells may contribute to SARS-CoV-2 variant control

Authors

Hiroshi Ishii, Takushi Nomura, Hiroyuki Yamamoto, ..., Yuriko Suzaki, Yasushi Ami, Tetsuro Matano

Correspondence

tmatano@nih.go.jp

In brief

Ishii et al. show neutralization-independent SARS-CoV-2 control associated with vaccine-induced CD8$^+$ T cell responses, indicating that virus-specific CD8$^+$ T cell induction by intranasal vaccination can result in SARS-CoV-2 control. Results highlight the potential of vaccine-induced CD8$^+$ T cell responses to contribute to the control of SARS-CoV-2 variants.

Ishii et al., 2022, Cell Reports Medicine *3*, 100520
February 15, 2022
https://doi.org/10.1016/j.xcrm.2022.100520

CellPress

Cell Reports Medicine

CellPress
OPEN ACCESS

Report

Neutralizing-antibody-independent SARS-CoV-2 control correlated with intranasal-vaccine-induced CD8+ T cell responses

Hiroshi Ishii,[1,9] Takushi Nomura,[1,9] Hiroyuki Yamamoto,[1] Masako Nishizawa,[1] Trang Thi Thu Hau,[1] Shigeyoshi Harada,[1] Sayuri Seki,[1] Midori Nakamura-Hoshi,[1] Midori Okazaki,[1] Sachie Daigen,[1] Ai Kawana-Tachikawa,[1,2,3] Noriyo Nagata,[4] Naoko Iwata-Yoshikawa,[4] Nozomi Shiwa,[4] Tadaki Suzuki,[4] Eun-Sil Park,[5] Maeda Ken,[5] Taishi Onodera,[6] Yoshimasa Takahashi,[6] Kohji Kusano,[7] Ryutaro Shimazaki,[7] Yuriko Suzaki,[8] Yasushi Ami,[8] and Tetsuro Matano[1,2,3,10,*]

[1]AIDS Research Center, National Institute of Infectious Diseases, Tokyo 162-8640, Japan
[2]Institute of Medical Science, University of Tokyo, Tokyo 108-8639, Japan
[3]Joint Research Center for Human Retrovirus Infection, Kumamoto University, Kumamoto 860-0811, Japan
[4]Department of Pathology, National Institute of Infectious Diseases, Tokyo 162-8640, Japan
[5]Department of Veterinary Science, National Institute of Infectious Diseases, Tokyo 162-8640, Japan
[6]Research Center for Drug and Vaccine Development, National Institute of Infectious Diseases, Tokyo 162-8640, Japan
[7]ID Pharma Co., Ltd., Ibaraki 300-2611, Japan
[8]Management Department of Biosafety, Laboratory Animal, and Pathogen Bank, National Institute of Infectious Diseases, Tokyo 162-8640, Japan
[9]These authors contributed equally
[10]Lead contact
*Correspondence: tmatano@nih.go.jp
https://doi.org/10.1016/j.xcrm.2022.100520

SUMMARY

Effective vaccines are essential for the control of the coronavirus disease 2019 (COVID-19) pandemic. Currently developed vaccines inducing severe acute respiratory syndrome coronavirus 2 (SARS-CoV-2) spike (S)-antigen-specific neutralizing antibodies (NAbs) are effective, but the appearance of NAb-resistant S variant viruses is of great concern. A vaccine inducing S-independent or NAb-independent SARS-CoV-2 control may contribute to containment of these variants. Here, we investigate the efficacy of an intranasal vaccine expressing viral non-S antigens against intranasal SARS-CoV-2 challenge in cynomolgus macaques. Seven vaccinated macaques exhibit significantly reduced viral load in nasopharyngeal swabs on day 2 post-challenge compared with nine unvaccinated controls. The viral control in the absence of SARS-CoV-2-specific NAbs is significantly correlated with vaccine-induced, viral-antigen-specific CD8+ T cell responses. Our results indicate that CD8+ T cell induction by intranasal vaccination can result in NAb-independent control of SARS-CoV-2 infection, highlighting a potential of vaccine-induced CD8+ T cell responses to contribute to COVID-19 containment.

INTRODUCTION

Coronavirus disease 2019 (COVID-19), caused by severe acute respiratory syndrome coronavirus 2 (SARS-CoV-2), has rapidly spread, resulting in a pandemic. SARS-CoV-2 transmission that can occur from asymptomatic infected individuals is difficult to control.[1] Development of an effective vaccine is key for the control of the COVID-19 pandemic. Several effective vaccines using mRNAs or viral vectors have been rapidly developed and are currently in clinical use.[2–5] Intramuscular administration of these vaccines elicits effective anti-SARS-CoV-2 neutralizing antibodies (NAbs), showing protective efficacy against COVID-19 onset and progression. Antibodies targeting the receptor-binding domain of the spike (S) antigen play a central role in virus neutralization.[6,7]

However, reports on SARS-CoV-2 variants have recently accumulated, and the appearance of NAb-resistant S variant viruses is of great concern.[8–10] For example, B.1.351 (β variant), a variant of concern (VOC), has shown reduced sensitivity to neutralization not only by convalescent plasma of COVID-19 patients but also by plasma from vaccinated individuals.[11–13] Hence, there is a demand for the development of a vaccine inducing effective immune responses against these NAb-resistant variants.[14,15]

While possible cross-reactivity of vaccine-induced NAb responses to variants has been indicated,[16–19] induction of virus-specific T cell responses may be an alternative vaccine strategy to control VOC epidemics. Involvement of virus-specific T cell responses in the control of SARS-CoV-2 infection has been suggested.[20,21] Early induction of functional virus-specific CD8+ T cell responses has been observed in convalescent COVID-19 individuals, implying contribution of CD8+ T cells in SARS-CoV-2 control.[22] Whereas CD8+ depletion in rhesus macaques did not solely lead to viral control failure or severe disease

progression in SARS-CoV-2 infection,[23,24] $CD8^+$ depletion prior to SARS-CoV-2 re-infection in rhesus macaques resulted in partial abrogation of protection, suggesting the potential of $CD8^+$ T cells to augment antibody-mediated viral control.[25] Induction of SARS-CoV-2-specific T cell responses, including those reactive to VOCs, has been shown in several vaccines,[2,4,19,26–29] while these vaccines were not S antigen free and also induced S-specific antibodies. Thus, T cell responses may play a role in vaccine efficacy, but the potential of vaccine-induced T cell responses to prevent SARS-CoV-2 infection in the absence of S-specific antibodies remains unclear.

In the present study, we investigated the protective efficacy of an intranasal S-free vaccine inducing T cell responses against SARS-CoV-2 challenge in cynomolgus macaques. Our results revealed significant association of viral suppression with vaccine-induced $CD8^+$ T cell responses, indicating that $CD8^+$ T cell induction by intranasal vaccination can result in S-independent or NAb-independent control of SARS-CoV-2 infection.

RESULTS

Induction of T cell responses targeting SARS-CoV-2 N, M, and E antigens by vaccination

We constructed plasmid DNAs expressing nucleocapsid (N), membrane (M), and envelope (E) antigens (pcDNA-N, pcDNA-M, and pcDNA-E, respectively) and a replication-incompetent F-deleted Sendai virus vector[30] expressing N, M, and E (SeV-NME) for vaccination. We attempted two vaccine protocols in this study (Table S1). Three cynomolgus macaques (V11, V12, and V13) received intramuscular vaccination (prime) with pcDNA-N, pcDNA-M, and pcDNA-E twice on days 0 and 4 and intranasal vaccination (boost) with SeV-NME at week 5. The other four cynomolgus macaques (V14, V15, V16, and V17) received intranasal SeV-NME vaccination twice with a 5-week interval.

Vaccine-induced SARS-CoV-2 N-, M-, and E-specific T cell responses were measured by flow cytometric analysis of interferon-γ (IFN-γ) induction after specific stimulation using panels of overlapping peptides spanning the N, M, and E amino acid sequences, respectively (Figures S1A and S1B). We confirmed that these T cell responses were undetectable before vaccination in the vaccinated macaques (Figure S1C). These T cell responses were also undetectable before challenge in the unvaccinated macaques that were used in the SARS-CoV-2 challenge experiment described in the next section (Figure S1D). The sum of N-specific, M-specific, and E-specific T cell frequencies is shown as NME-specific T cell responses (Figure 1). Analysis using peripheral blood mononuclear cells (PBMCs) 2 weeks after the last vaccination confirmed that NME-specific T cell responses were elicited in all seven immunized macaques, although efficiently in some animals, but not in others. In macaques V11, V12, and V13, NME-specific T cell responses were undetectable after the DNA prime (Figure S1E) but induced after the SeV-NME boost. It has been indicated that such heterologous prime-boost mostly can be more immunogenic than homologous prime-boost,[31] and macaques V11 and V12 efficiently induced NME-specific $CD4^+$ T cell and $CD8^+$ T cell responses, whereas NME-specific $CD4^+$ T cell responses were lower and $CD8^+$ T cell responses were undetectable in macaque V13. In four macaques (V14, V15, V16, and V17) receiving SeV-NME twice, NME-specific $CD4^+$ T cell and $CD8^+$ T cell responses were detectable in three macaques except for V17, which showed only marginal NME-specific $CD4^+$ T cell responses. SeV-specific $CD4^+$ T cell and $CD8^+$ T cell responses were efficiently induced in all of the vaccinated macaques (Figure S2A). By enzyme-linked immunosorbent assay (ELISA), anti-SARS-CoV-2 N antibodies were detected in post-vaccination plasma of all the vaccinated macaques (Figure S2B), whereas anti-M and anti-E antibodies were detectable only in macaque V16 (Figure S2C) and in macaques V16 and V17 (Figure S2D), respectively.

Reduction in viral loads in the vaccinated macaques compared with the unvaccinated controls after SARS-CoV-2 challenge

These vaccinated macaques were intranasally challenged with 10^5 50% tissue culture infective doses ($TCID_{50}$) of SARS-CoV-2 wk-521 (2019-nCoV/Japan/TY/WK-521/2020)[32] at week 6 after the last vaccination. NME-specific $CD4^+$ T cell and $CD8^+$ T cell responses were detectable just before challenge in five and three macaques, respectively (Figure 1). None of these vaccinated macaques induced anti-SARS-CoV-2 NAb responses before SARS-CoV-2 challenge (Table S2). Four unvaccinated cynomolgus macaques (N031, N032, N041, and N042) were also intranasally challenged with 10^5 $TCID_{50}$ of SARS-CoV-2. Data on additional five cynomolgus macaques intranasally infected with 10^5 $TCID_{50}$ of the same SARS-CoV-2 stock in our previous study[23] were used as historical unvaccinated controls (Table S1).

In the unvaccinated controls (n = 9), the geometric mean of viral RNA levels in nasopharyngeal swabs on day 2 post-challenge was 1.1×10^8 copies/swab (Figure 2A). One macaque N032 showed 5.6×10^5 copies/swab, but the remaining eight macaques had 6.9×10^7–1.1×10^9 copies/swab. In contrast, six of the seven vaccinated macaques showed less than 8.7×10^6 copies/swab of viral RNAs (Figure 2A). Comparison revealed significantly lower viral RNA levels in nasopharyngeal swabs on day 2 post-challenge in the vaccinated than the unvaccinated macaques ($p = 0.0311$ by Mann-Whitney U test; Figure 2B). Viral subgenomic RNAs (sgRNAs) in nasopharyngeal swabs were detected on day 2 post-challenge in eight of the nine unvaccinated controls but undetectable in six of the seven vaccinated macaques (Figure 2C), exhibiting significant reduction in the viral sgRNA levels in the vaccinated macaques compared with the unvaccinated controls ($p = 0.0039$ by Mann-Whitney U test; Figure 2D). Virus recovery from the nasopharyngeal swabs was consistent with viral RNA levels described above (Figure 2E), and a significant reduction in viral titers on day 2 post-challenge was observed in the vaccinated macaques compared with the unvaccinated ($p = 0.0240$ by Mann-Whitney U test; Figure 2F). These results indicate protective efficacy of the vaccination against intranasal SARS-CoV-2 challenge.

Correlation between viral control and vaccine-induced, NME-specific $CD8^+$ T cell responses

We then investigated immune correlates for this protective efficacy in the seven vaccinated macaques. Remarkably, analysis

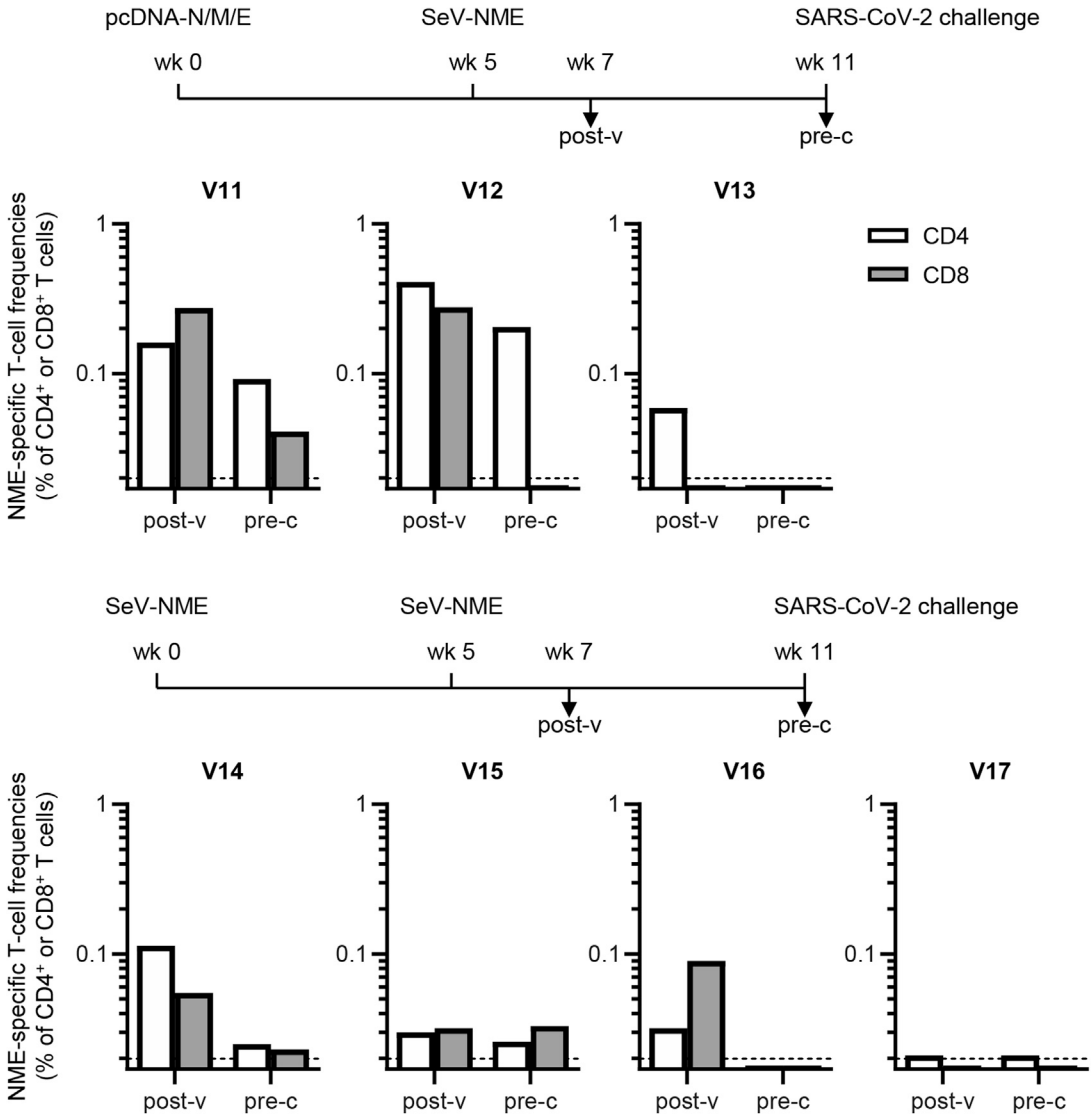

Figure 1. SARS-CoV-2 NME-specific T cell responses after vaccination

SARS-CoV-2 N-, M-, and E-antigen-specific $CD4^+$ T cell and $CD8^+$ T cell responses were examined using PBMCs obtained 2 weeks after the last vaccination (post-v) and just before SARS-CoV-2 challenge (pre-c: 6 weeks after the last vaccination). N-, M-, and E-specific T cell frequencies were calculated by subtracting nonspecific IFN-γ^+ T cell frequencies from those after stimulation with overlapping peptides spanning the SARS-CoV-2 N, M, and E amino acid sequences, respectively. The sums of N-, M-, and E-specific $CD4^+$ T cell and $CD8^+$ T cell frequencies above the cutoff value (0.02%) are shown as NME-specific $CD4^+$ T cell (open box) and $CD8^+$ T cell (closed box) responses, respectively. Macaques V11, V12, and V13 shown in upper panels received pcDNA-N/M/E prime followed by SeV-NME boost. Macaques V14, V15, V16, and V17 shown in lower panels received SeV-NME vaccination twice. See also Figure S1.

revealed a significant inverse correlation between viral RNA levels in nasopharyngeal swabs on day 2 post-challenge and NME-specific $CD8^+$ T cell responses 2 weeks after the last vaccination ($p = 0.0040$; $r = -0.9550$ by Spearman's test; Figure 3A). In contrast, no correlation was observed between the viral RNA levels and vaccine-induced, NME-specific $CD4^+$ T cell responses. Further analysis showed significant inverse correlation between viral RNA levels in nasopharyngeal swabs on day 2 post-challenge and vaccine-induced, N-antigen-specific $CD8^+$ T cell responses that were predominant in vaccine-induced, NME-specific $CD8^+$ T cell responses ($p = 0.0254$; $r = -0.8365$ by Spearman's test; Figure S3A). We confirmed no significant correlation between the viral RNA levels and vaccine-induced, SeV-specific $CD4^+$ T cell or $CD8^+$ T cell responses (Figure S3B). No significant correlation was observed between viral RNA levels in nasopharyngeal swabs on day 2 post-challenge and vaccine-induced anti-N antibody levels (Figure S3C), although significant correlation between the anti-N antibody levels and vaccine-induced N-antigen-specific $CD8^+$ T cell responses was indicated (Figure S3D). Anti-M and anti-E antibodies post-vaccination were detectable in only one or two vaccinated macaques but undetectable in macaques V11 and V12 that showed the top two

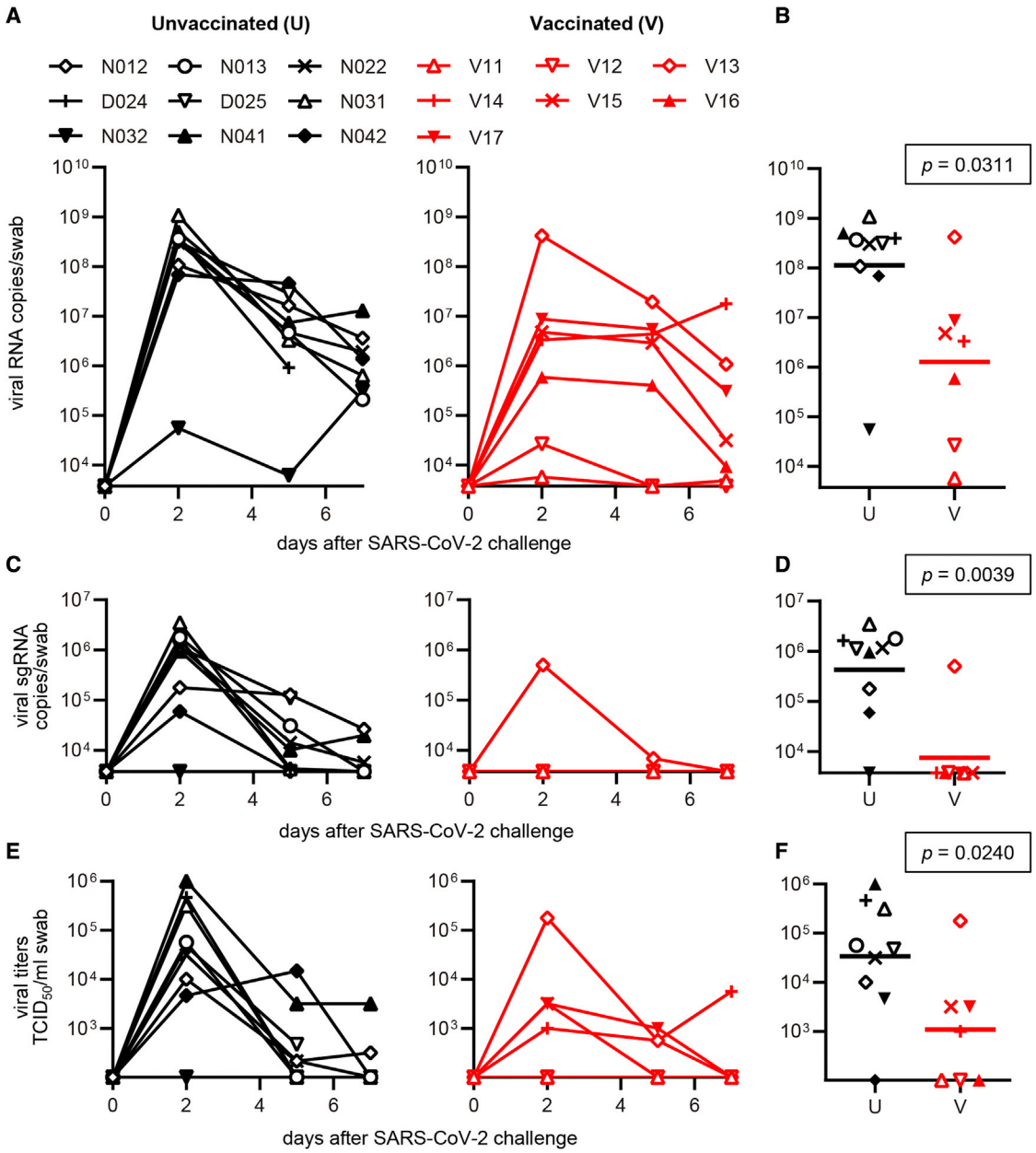

Figure 2. Viral loads in nasopharyngeal swabs after intranasal SARS-CoV-2 challenge

(A) Changes in viral RNA levels in nasopharyngeal swabs after SARS-CoV-2 challenge in the nine unvaccinated controls (U; black; left panel) and the seven vaccinated macaques (V; red; right panel). Data on three macaques (V11, V12, and V13) vaccinated with pcDNA-N/M/E prime/SeV-NME boost are indicated by open symbols. Data on day 0 are those just before challenge. Viral RNA levels less than 3×10^3 copies/swab were undetectable.

(B) Comparison of viral RNA levels on day 2 post-challenge between unvaccinated (U) and vaccinated (V) macaques. Vaccinated macaques showed significantly lower viral RNA levels compared with the unvaccinated controls (by Mann-Whitney U test).

(C) Changes in viral sgRNA levels in nasopharyngeal swabs in U and V. Viral sgRNA levels less than 3×10^3 copies/swab were undetectable.

(D) Comparison of viral sgRNA levels on day 2 between U and V. Vaccinated macaques showed significantly lower viral sgRNA levels compared with the unvaccinated controls (by Mann-Whitney U test).

(E) Changes in viral titers in nasopharyngeal swabs in U and V. Swab samples with virus titers greater than 1×10^2 $TCID_{50}$/swab were considered positive.

(F) Comparison of viral titers on day 2 between U and V. Vaccinated macaques showed significantly lower viral titers compared with the unvaccinated controls (by Mann-Whitney U test). Data on historical unvaccinated controls N012, N013, N022, D024, and D025 were described before.[23]

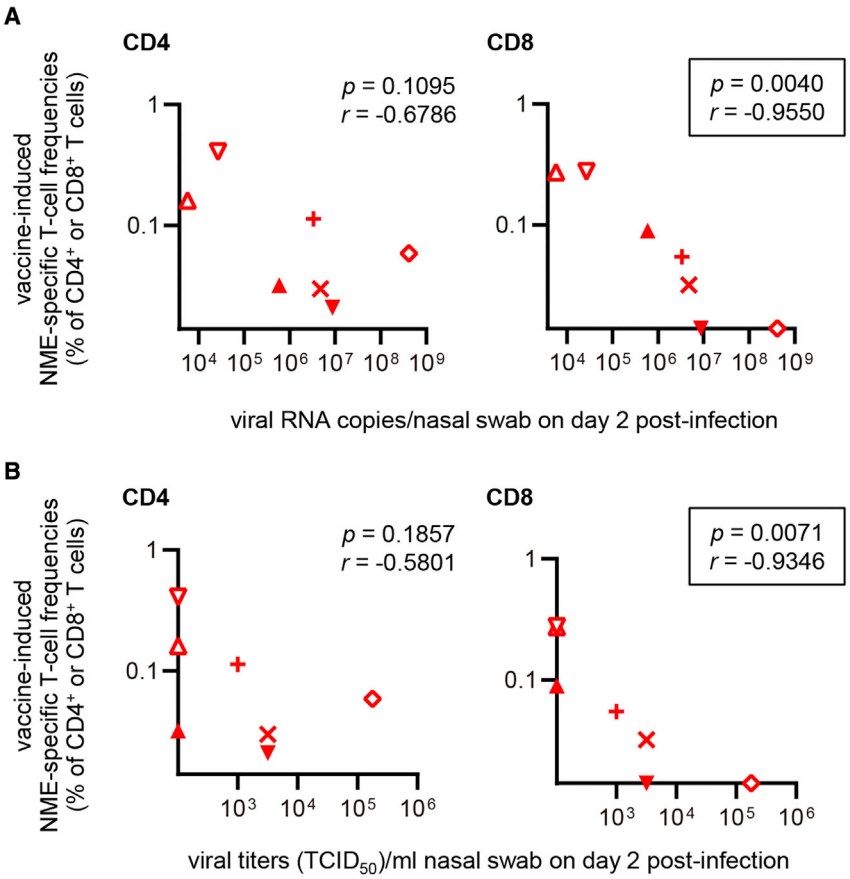

Figure 3. Correlation of SARS-CoV-2 control with vaccine-induced T cell responses

(A) Correlation analyses between viral RNA levels in nasopharyngeal swabs on day 2 post-challenge and NME-specific $CD4^+$ T cell (left panel) and $CD8^+$ T cell (right panel) frequencies in PBMCs 2 weeks after the last vaccination in the seven vaccinated macaques. Significant inverse correlation between the viral RNA levels and vaccine-induced, NME-specific $CD8^+$ T cell responses was observed (by Spearman's test).

(B) Correlation analyses between viral titers in nasopharyngeal swabs on day 2 post-challenge and NME-specific $CD4^+$ T cell (left panel) and $CD8^+$ T cell (right panel) frequencies in PBMCs 2 weeks after the last vaccination. Significant inverse correlation between the viral titers and vaccine-induced, NME-specific $CD8^+$ T cell responses was observed (by Spearman's test).

lowest viral RNA levels in nasopharyngeal swabs on day 2 post-challenge (Figures S2C and S2D). Significant inverse correlation was observed between NME-specific $CD8^+$ T cell responses 2 weeks after the last vaccination and viral RNA levels in nasopharyngeal swabs on day 5 ($p = 0.0044$; $r = -0.9455$ by Spearman's test), but not on day 7 ($p = 0.0508$; $r = -0.7748$ by Spearman's test) post-challenge (Figures S3E and S3F).

Viral titers in nasopharyngeal swabs on day 2 post-challenge were also inversely correlated with the vaccine-induced, NME-specific $CD8^+$ T cell responses ($p = 0.0071$; $r = -0.9346$ by Spearman's test; Figure 3B). The three vaccinated macaques (V11, V12, and V16) that exhibited the top three highest frequencies of vaccine-induced, NME-specific $CD8^+$ T cells showed no virus recovery post-challenge (Figure 2E).

Analysis of tissues obtained at necropsy on day 7 or 9 post-challenge detected viral sgRNA in the pharyngeal mucosa and/or retropharyngeal lymph nodes (RPLNs) of the four unvaccinated controls (Table S3). It should be noted that sgRNA in the pharyngeal mucosa was detected even in macaque N032, despite low viral RNA levels in nasopharyngeal swabs. In contrast, viral sgRNA was undetectable in the pharyngeal mucosa and RPLNs in the three vaccinated macaques (V11, V12, and V16) that exhibited the top three highest frequencies of vaccine-induced NME-specific $CD8^+$ T cells. Viral RNA levels in nasopharyngeal swabs on day 7 post-challenge were greater than 10^5 copies/swab in all of the unvaccinated macaques but less than 10^4 copies/swab in these three vaccinated macaques (Figure 2A). Thus, in these three, sgRNA was undetectable not only in nasopharyngeal swabs but also in the pharyngeal mucosa and RPLNs obtained at necropsy (Table S3).

Analysis using PBMCs on day 7 post-challenge detected NME-specific $CD8^+$ T cell responses in five of the seven vaccinated macaques (Figure 4A). In contrast, analysis using lymphocytes derived from the submandibular lymph nodes (SMLNs) obtained at necropsy on day 7 or 9 post-challenge detected NME-specific $CD8^+$ T cell responses in all of the seven vaccinated macaques (Figure 4B). The NME-specific $CD8^+$ T cell frequencies in SMLNs in the vaccinated were significantly higher than the four unvaccinated macaques (N031, N032, N041, and N042; $p = 0.0394$ by Mann-Whitney U test). NME-specific $CD8^+$ T cell responses in the lung were detected in six vaccinated macaques except for V13, showing the highest viral RNA level in the nasopharyngeal swab on day 2 (Figure 4C).

DISCUSSION

This study is the first to show a significant association between SARS-CoV-2 control and vaccine-induced $CD8^+$ T cell responses in the absence of NAbs, indicating that induction of SARS-CoV-2-specific $CD8^+$ T cell responses by intranasal vaccination can contribute to the control of SARS-CoV-2 infection. We recognize that induction of T cell responses by our vaccine is not consistently efficient and two vaccine protocols were attempted in the present study, but thereby, the vaccination resulted in various levels of T cell responses and viral protection, which enabled us to determine the important immune correlates. Further optimization of an intranasal vaccine protocol using more immunogenic delivery systems would lead to efficient and durable SARS-CoV-2-specific $CD8^+$ T cell induction, possibly resulting in enhanced protection, which could bring SARS-CoV-2

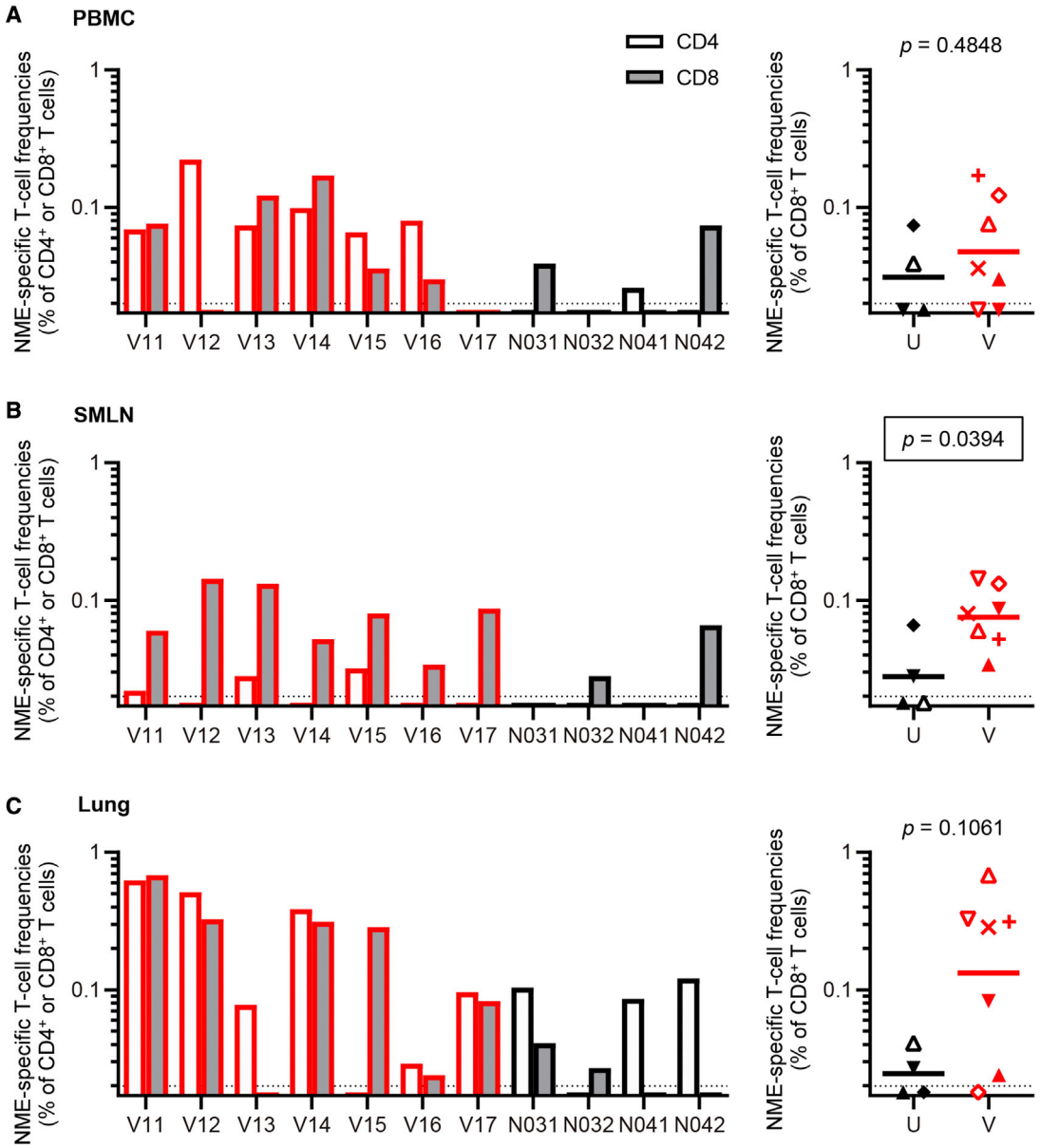

Figure 4. NME-specific T cell responses after SARS-CoV-2 challenge

NME-specific CD4$^+$ T cell (open box) and CD8$^+$ T cell (closed box) frequencies in PBMCs, the submandibular lymph nodes (SMLNs), and the lung post-challenge in the four unvaccinated (U) and the seven vaccinated (V) macaques. Data on the five historical unvaccinated controls were unavailable.

(A) NME-specific CD4$^+$ T cell and CD8$^+$ T cell frequencies in PBMCs on day 7 post-challenge. Comparison of NME-specific CD8$^+$ T cell frequencies in PBMCs between U and V is shown in the right panel.

(B) NME-specific CD4$^+$ T cell and CD8$^+$ T cell frequencies in SMLNs obtained at necropsy on day 7 or 9 post-challenge. Comparison of NME-specific CD8$^+$ T cell frequencies in SMLNs between U and V is shown in the right panel. Vaccinated macaques showed significantly higher CD8$^+$ T cell frequencies compared with the unvaccinated controls (by Mann-Whitney U test).

(C) NME-specific CD4$^+$ T cell and CD8$^+$ T cell frequencies in the lung obtained at necropsy. Comparison of NME-specific CD8$^+$ T cell frequencies in the lung between U and V is shown in the right panel.

variants under control. Furthermore, our results might support a notion that CD8$^+$ T cell responses induced by currently developed S-expressing vaccines may contribute to variant control.

The present study showed significant inverse correlation of viral RNA levels in nasopharyngeal swabs on day 2 post-challenge with vaccine-induced, NME-specific CD8$^+$ T cell, but not CD4$^+$ T cell responses, indicating the association of viral control with vaccine-induced, NME-specific CD8$^+$ T cell responses (Figure 3). Viral control was not associated with vaccine-induced antibodies nor SeV-specific T cell responses, which might reflect vaccine-induced nonspecific immune responses (Figures S3B and S3C). Significant inverse correlation was observed between

vaccine-induced, NME-specific CD8$^+$ T cell responses and viral RNA levels in nasopharyngeal swabs on day 5 ($p = 0.0044$ in Figure S3E), but not on day 7 ($p = 0.0508$; Figure S3F). It may reflect the following two points. First, the three vaccinated macaques (V11, V12, and V16) that exhibited the top three highest vaccine-induced CD8$^+$ T cell responses efficiently controlled SARS-CoV-2 replication, indicating the impact of vaccine-induced CD8$^+$ T cell responses on viral control. Second, in the other four macaques with inefficient vaccine-induced CD8$^+$ T cell responses and inefficient suppression of viral replication post-challenge, viral replication 1 week post-infection could be affected also by vaccine-independent immune responses induced post-infection.

Vaccine-induced, NME-specific CD8$^+$ T cell responses detected in PBMCs may not directly work for the rapid viral control after the intranasal SARS-CoV-2 challenge. However, our finding of the immuno-correlate might imply direct contribution of vaccine-induced mucosal CD8$^+$ T cell responses around the pharyngeal mucosa to rapid viral control. It is speculated that vaccine-induced peripheral NME-specific CD8$^+$ T cell responses around the peak (rather than just before challenge) are indicative of efficient mucosal NME-specific CD8$^+$ T cell responses around the pharyngeal mucosa. Indeed, our previous study showed the potential of intranasal immunization with an SeV vector expressing simian immunodeficiency virus Gag to induce Gag-specific T cell responses in the tonsil, nasal mucosa, and its primary lymph nodes (RPLN and SMLN).[33,34]

In our cynomolgus model of SARS-CoV-2 infection, kinetics of viral sgRNA levels in nasopharyngeal swabs (geometric mean on day 2: 4.3×10^5 copies/swab) in unvaccinated controls were similar to those for evaluation of NAb-inducing vaccine efficacy in other groups.[26,27] Thus, our results of undetectable viral sgRNAs in nasopharyngeal swabs from six of the seven vaccinated macaques suggest that the reduction in nasopharyngeal viral load by efficient NME-specific CD8$^+$ T cell responses is comparable with that by effective NAb-inducing vaccines.[26,27]

In addition to the data on viral load in nasopharyngeal swabs, we had data on viral sgRNA in the pharyngeal mucosa, RPLN, and the lung obtained at necropsy (Table S3). Viral sgRNA in the lung was undetectable in all the unvaccinated and vaccinated macaques, while bronchoalveolar lavage (BAL) was unexamined. Viral sgRNA in RPLN was detectable in three of the four unvaccinated macaques but undetectable in all the seven vaccinated. Viral sgRNA in the pharyngeal mucosa was detected in the four vaccinated macaques (V13, V14, V15, and V17) with inefficient vaccine-induced, NME-specific CD8$^+$ T cell responses but undetectable in the three vaccinated macaques (V11, V12, and V16) that exhibited the top three highest frequencies of vaccine-induced, NME-specific CD8$^+$ T cells, supporting our conclusion of association of viral control with vaccine-induced CD8$^+$ T cell responses. These three vaccinated macaques with efficient vaccine-induced, NME-specific CD8$^+$ T cell responses controlled SARS-CoV-2 replication without detectable virus recovery from nasopharyngeal swabs or sgRNAs in the pharyngeal mucosa. Although complete protection may be difficult, the rapid reduction in nasopharyngeal viral load that was shown in the present study would be important for inhibition of SARS-CoV-2 transmission from vaccinated but infected individuals, which could be a key for the control of COVID-19 pandemic.

Viral sgRNAs were undetectable in the lung for all animals, regardless of vaccination status, as described above (Table S3). However, histopathological analysis of the lung obtained at necropsy on days 7 or 9 post-challenge confirmed lesions in multiple lobes in all of the seven vaccinated and the four unvaccinated macaques (Figure S4). Epithelial degeneration and/or infiltration of macrophages, neutrophils, eosinophils, or mononuclear cells were detected, whereas no severe bronchiolitis or intestinal pulmonary inflammation was observed. It is speculated that even the vaccinated macaques efficiently inducing NME-specific CD8$^+$ T cell responses allowed SARS-CoV-2 infection in the lung but rapidly exerted immune responses, resulting in prompt control of viral replication. However, we should be careful about a possibility that virus-specific T cell induction by vaccination can result in aberrant pulmonary inflammation post-virus exposure, which could be a next subject to be addressed.

In summary, this pre-clinical study presents evidence indicating that induction of SARS-CoV-2-specific CD8$^+$ T cell responses by intranasal vaccination can result in the control of SARS-CoV-2 infection in the absence of NAbs. A rapid reduction in nasopharyngeal viral load could greatly contribute to the control of SARS-CoV-2 transmission. Although careful assessment of possible vaccine effect on pulmonary inflammation may be required, the present study highlights the potential of vaccine-induced T cell responses to contribute to the control of SARS-CoV-2 variants, providing a rationale of facilitating studies on vaccines inducing T cells in addition to NAbs for COVID-19 containment.

Limitations of the study

This study showed a significant association between SARS-CoV-2 control and vaccine-induced CD8$^+$ T cell responses. However, the vaccine-induced, NME-specific CD8$^+$ T cell responses detected in PBMCs may not directly work for the rapid viral control after the intranasal SARS-CoV-2 challenge. Contribution of vaccine-induced mucosal CD8$^+$ T cell responses around the pharyngeal mucosa to rapid viral control is speculated, but we had no data on mucosal CD8$^+$ T cell responses just before challenge in the present study. It is difficult to obtain sufficient lymphocytes around the pharyngeal mucosa by biopsy just before challenge for T cell analysis. Analysis of samples obtained from the pharyngeal mucosa by necropsy before challenge and/or BAL-derived lymphocytes that may be useful to investigate T cell responses in the lung could be the next issue.

STAR★METHODS

Detailed methods are provided in the online version of this paper and include the following:

- KEY RESOURCES TABLE
- RESOURCE AVAILABILITY
  - Lead contact
  - Materials availability
  - Data and code availability
- EXPERIMENTAL MODEL AND SUBJECT DETAILS

SUPPLEMENTAL INFORMATION

Supplemental information can be found online at https://doi.org/10.1016/j.xcrm.2022.100520.

ACKNOWLEDGMENTS

We thank S. Matsuyama and M. Takeda for providing SARS-CoV-2 wk-521 and Vero E6/TMPRSS2 cells, H. Ohashi and K. Watashi for providing Vero cells, and S. Fukushi for his help. We also thank M. de Souza for editing the paper. This work was supported by Japan Agency for Medical Research and Development (AMED [JP19fk0108104 to A.K.-T. and JP20nk0101601, JP20jm0110012, JP21fk0410035, JP21fk0108125, and JP21jk0210002 to T.M.]) and the Ministry of Education, Culture, Sports, Science and Technology (MEXT) in Japan (JSPS Grants-in-Aid for Scientific Research [21H02745 to T.M.]).

AUTHOR CONTRIBUTIONS

H.I., T.N., and T.M. conceived and designed the experiments. K.K. and R.S. produced SeV vectors. H.I., T.N., H.Y., M.N., T.T.T.H., S.H., S.S., M.N.-H., N.N., N.I.-Y., N.S., T.S., Y.S., and Y.A. performed macaque experiments. H.I., T.N., H.Y., T.T.T.H., S.H., S.S., M.O., S.D., A.K.-T., E.-S.P., K.M., T.O., and Y.T. performed virological and immunological analyses. N.N., N.I.-Y., N.S., and T.S. performed pathological analyses. H.I., T.N., and T.M. analyzed the data. H.I., T.N., and T.M. wrote the paper.

DECLARATION OF INTERESTS

H.I., K.K., R.S., and T.M. are the inventors on Patent Cooperation Treaty (PCT) application for SeV-NME vaccine. The authors declare no other competing interests.

Received: September 8, 2021
Revised: November 27, 2021
Accepted: January 13, 2022
Published: January 19, 2022

REFERENCES

1. Moghadas, S.M., Fitzpatrick, M.C., Sah, P., Pandey, A., Shoukat, A., Singer, B.H., and Galvani, A.P. (2020). The implications of silent transmission for the control of COVID-19 outbreaks. Proc. Natl. Acad. Sci. U S A *117*, 17513–17515.
2. Polack, F.P., Thomas, S.J., Kitchin, N., Absalon, J., Gurtman, A., Lockhart, S., Perez, J.L., Pérez Marc, G., Moreira, E.D., Zerbini, C., et al. (2020). Safety and efficacy of the BNT162b2 mRNA covid-19 vaccine. N. Engl. J. Med. *383*, 2603–2615.
3. Baden, L.R., El Sahly, H.M., Essink, B., Kotloff, K., Frey, S., Novak, R., Diemert, D., Spector, S.A., Rouphael, N., Creech, C.B., et al. (2021). Efficacy and safety of the mRNA-1273 SARS-CoV-2 vaccine. N. Engl. J. Med. *384*, 403–416.
4. Voysey, M., Clemens, S., Madhi, S.A., Weckx, L.Y., Folegatti, P.M., Aley, P.K., Angus, B., Baillie, V.L., Barnabas, S.L., Bhorat, Q.E., et al. (2021). Safety and efficacy of the ChAdOx1 nCoV-19 vaccine (AZD1222) against SARS-CoV-2: an interim analysis of four randomised controlled trials in Brazil, South Africa, and the UK. Lancet *397*, 99–111.
5. Sadoff, J., Gray, G., Vandebosch, A., Cárdenas, V., Shukarev, G., Grinsztejn, B., Goepfert, P.A., Truyers, C., Fennema, H., Spiessens, B., et al. (2021). Safety and efficacy of single-dose Ad26.COV2.S vaccine against covid-19. N. Engl. J. Med. *384*, 2187–2201.
6. Barnes, C.O., Jette, C.A., Abernathy, M.E., Dam, K.A., Esswein, S.R., Gristick, H.B., Malyutin, A.G., Sharaf, N.G., Huey-Tubman, K.E., Lee, Y.E., et al. (2020). SARS-CoV-2 neutralizing antibody structures inform therapeutic strategies. Nature *588*, 682–687.
7. Yuan, M., Liu, H., Wu, N.C., and Wilson, I.A. (2021). Recognition of the SARS-CoV-2 receptor binding domain by neutralizing antibodies. Biochem. Biophys. Res. Commun. *538*, 192–203.
8. Tegally, H., Wilkinson, E., Giovanetti, M., Iranzadeh, A., Fonseca, V., Giandhari, J., Doolabh, D., Pillay, S., San, E.J., Msomi, N., et al. (2021). Detection of a SARS-CoV-2 variant of concern in South Africa. Nature *592*, 438–443.
9. Washington, N.L., Gangavarapu, K., Zeller, M., Bolze, A., Cirulli, E.T., Schiabor Barrett, K.M., Larsen, B.B., Anderson, C., White, S., Cassens, T., et al. (2021). Emergence and rapid transmission of SARS-CoV-2 B.1.1.7 in the United States. Cell *184*, 2587–2594.e7.
10. Boehm, E., Kronig, I., Neher, R.A., Eckerle, I., Vetter, P., and Kaiser, L.; Geneva Centre for Emerging Viral Diseases (2021). Novel SARS-CoV-2 variants: the pandemics within the pandemic. Clin. Microbiol. Infect. *27*, 1109–1117.
11. Zhou, D., Dejnirattisai, W., Supasa, P., Liu, C., Mentzer, A.J., Ginn, H.M., Zhao, Y., Duyvesteyn, H., Tuekprakhon, A., Nutalai, R., et al. (2021). Evidence of escape of SARS-CoV-2 variant B.1.351 from natural and vaccine-induced sera. Cell *184*, 2348–2361.e6.
12. Hoffmann, M., Arora, P., Groß, R., Seidel, A., Hörnich, B.F., Hahn, A.S., Krüger, N., Graichen, L., Hofmann-Winkler, H., Kempf, A., et al. (2021). SARS-CoV-2 variants B.1.351 and P.1 escape from neutralizing antibodies. Cell *184*, 2384–2393.e12.
13. Wang, P., Nair, M.S., Liu, L., Iketani, S., Luo, Y., Guo, Y., Wang, M., Yu, J., Zhang, B., Kwong, P.D., et al. (2021). Antibody resistance of SARS-CoV-2 variants B.1.351 and B.1.1.7. Nature *593*, 130–135.
14. Krause, P.R., Fleming, T.R., Longini, I.M., Peto, R., Briand, S., Heymann, D.L., Beral, V., Snape, M.D., Rees, H., Ropero, A.M., et al. (2021). SARS-CoV-2 variants and vaccines. N. Engl. J. Med. *385*, 179–186.
15. Tregoning, J.S., Flight, K.E., Higham, S.L., Wang, Z., and Pierce, B.F. (2021). Progress of the COVID-19 vaccine effort: viruses, vaccines and variants versus efficacy, effectiveness and escape. Nat. Rev. Immunol. *21*, 626–636.
16. Lopez Bernal, J., Andrews, N., Gower, C., Gallagher, E., Simmons, R., Thelwall, S., Stowe, J., Tessier, E., Groves, N., Dabrera, G., et al. (2021). Effectiveness of covid-19 vaccines against the B.1.617.2 (Delta) variant. N. Engl. J. Med. *385*, 585–594.
17. Pegu, A., O'Connell, S., Schmidt, S.D., O'Dell, S., Talana, C.A., Lai, L., Albert, J., Anderson, E., Bennett, H., Corbett, K.S., et al. (2021). Durability of mRNA-1273 vaccine-induced antibodies against SARS-CoV-2 variants. Science *373*, 1372–1377.
18. Urbanowicz, R.A., Tsoleridis, T., Jackson, H.J., Cusin, L., Duncan, J.D., Chappell, J.G., Tarr, A.W., Nightingale, J., Norrish, A.R., Ikram, A., et al. (2021). Two doses of the SARS-CoV-2 BNT162b2 vaccine enhances antibody responses to variants in individuals with prior SARS-CoV-2 infection. Sci. Transl. Med. *13*, eabj0847.
19. Yu, J., Tostanoski, L.H., Mercado, N.B., McMahan, K., Liu, J., Jacob-Dolan, C., Chandrashekar, A., Atyeo, C., Martinez, D.R., Anioke, T., et al.

(2021). Protective efficacy of Ad26.COV2.S against SARS-CoV-2 B.1.351 in macaques. Nature *596*, 423–427.

20. Peng, Y., Mentzer, A.J., Liu, G., Yao, X., Yin, Z., Dong, D., Dejnirattisai, W., Rostron, T., Supasa, P., Liu, C., et al. (2020). Broad and strong memory $CD4^+$ and $CD8^+$ T cells induced by SARS-CoV-2 in UK convalescent individuals following COVID-19. Nat. Immunol. *21*, 1336–1345.
21. Rydyznski Moderbacher, C., Ramirez, S.I., Dan, J.M., Grifoni, A., Hastie, K.M., Weiskopf, D., Belanger, S., Abbott, R.K., Kim, C., Choi, J., et al. (2020). Antigen-specific adaptive immunity to SARS-CoV-2 in acute COVID-19 and associations with age and disease severity. Cell *183*, 996–1012.e19.
22. Tan, A.T., Linster, M., Tan, C.W., Le Bert, N., Chia, W.N., Kunasegaran, K., Zhuang, Y., Tham, C., Chia, A., Smith, G., et al. (2021). Early induction of functional SARS-CoV-2-specific T cells associates with rapid viral clearance and mild disease in COVID-19 patients. Cell Rep. *34*, 108728.
23. Nomura, T., Yamamoto, H., Nishizawa, M., Hau, T., Harada, S., Ishii, H., Seki, S., Nakamura-Hoshi, M., Okazaki, M., Daigen, S., et al. (2021). Subacute SARS-CoV-2 replication can be controlled in the absence of $CD8^+$ T cells in cynomolgus macaques. PLoS Pathog. *17*, e1009668.
24. Hasenkrug, K.J., Feldmann, F., Myers, L., Santiago, M.L., Guo, K., Barrett, B.S., Mickens, K.L., Carmody, A., Okumura, A., Rao, D., et al. (2021). Recovery from acute SARS-CoV-2 infection and development of anamnestic immune responses in T cell-depleted rhesus macaques. mBio *12*, e0150321.
25. McMahan, K., Yu, J., Mercado, N.B., Loos, C., Tostanoski, L.H., Chandrashekar, A., Liu, J., Peter, L., Atyeo, C., Zhu, A., et al. (2021). Correlates of protection against SARS-CoV-2 in rhesus macaques. Nature *590*, 630–634.
26. Mercado, N.B., Zahn, R., Wegmann, F., Loos, C., Chandrashekar, A., Yu, J., Liu, J., Peter, L., McMahan, K., Tostanoski, L.H., et al. (2020). Single-shot Ad26 vaccine protects against SARS-CoV-2 in rhesus macaques. Nature *586*, 583–588.
27. Routhu, N.K., Cheedarla, N., Gangadhara, S., Bollimpelli, V.S., Boddapati, A.K., Shiferaw, A., Rahman, S.A., Sahoo, A., Edara, V.V., Lai, L., et al. (2021). A modified vaccinia Ankara vector-based vaccine protects macaques from SARS-CoV-2 infection, immune pathology, and dysfunction in the lungs. Immunity *54*, 542–556.e9.
28. Alter, G., Yu, J., Liu, J., Chandrashekar, A., Borducchi, E.N., Tostanoski, L.H., McMahan, K., Jacob-Dolan, C., Martinez, D.R., Chang, A., et al. (2021). Immunogenicity of Ad26.COV2.S vaccine against SARS-CoV-2 variants in humans. Nature *596*, 268–272.
29. Painter, M.M., Mathew, D., Goel, R.R., Apostolidis, S.A., Pattekar, A., Kuthuru, O., Baxter, A.E., Herati, R.S., Oldridge, D.A., Gouma, S., et al. (2021). Rapid induction of antigen-specific $CD4^+$ T cells is associated with coordinated humoral and cellular immune responses to SARS-CoV-2 mRNA vaccination. Immunity *54*, 2133–2142.e3.
30. Matano, T., Kobayashi, M., Igarashi, H., Takeda, A., Nakamura, H., Kano, M., Sugimoto, C., Mori, K., Iida, A., Hirata, T., et al. (2004). Cytotoxic T lymphocyte-based control of simian immunodeficiency virus replication in a preclinical AIDS vaccine trial. J. Exp. Med. *199*, 1709–1718.
31. Lu, S. (2009). Heterologous prime-boost vaccination. Curr. Opin. Immunol. *21*, 346–351.
32. Matsuyama, S., Nao, N., Shirato, K., Kawase, M., Saito, S., Takayama, I., Nagata, N., Sekizuka, T., Katoh, H., Kato, F., et al. (2020). Enhanced isolation of SARS-CoV-2 by TMPRSS2-expressing cells. Proc. Natl. Acad. Sci. U S A. *117*, 7001–7003.
33. Takeda, A., Igarashi, H., Nakamura, H., Kano, M., Iida, A., Hirata, T., Hasegawa, M., Nagai, Y., and Matano, T. (2003). Protective efficacy of an AIDS vaccine, a single DNA-prime followed by a single booster with a recombinant replication-defective Sendai virus vector, in a macaque AIDS model. J. Virol. *77*, 9710–9715.
34. Takeda, A., Igarashi, H., Kawada, M., Tsukamoto, T., Yamamoto, H., Inoue, M., Iida, A., Shu, T., Hasegawa, M., and Matano, T. (2008). Evaluation of the immunogenicity of replication-competent V-knocked-out and replication-defective F-deleted Sendai virus vector-based vaccines in macaques. Vaccine *26*, 6839–6843.
35. Li, H.O., Zhu, Y.F., Asakawa, M., Kuma, H., Hirata, T., Ueda, Y., Lee, Y.S., Fukumura, M., Iida, A., Kato, A., et al. (2000). A cytoplasmic RNA vector derived from nontransmissible Sendai virus with efficient gene transfer and expression. J. Virol. *74*, 6564–6569.
36. Ishii, H., Terahara, K., Nomura, T., Takeda, A., Okazaki, M., Yamamoto, H., Tokusumi, T., Shu, T., and Matano, T. (2020). A novel immunogen selectively eliciting $CD8^+$ T cells but not $CD4^+$ T cells targeting immunodeficiency virus antigens. J. Virol. *94*, e01876–19.
37. Shirato, K., Nao, N., Katano, H., Takayama, I., Saito, S., Kato, F., Katoh, H., Sakata, M., Nakatsu, Y., Mori, Y., et al. (2020). Development of genetic diagnostic methods for detection for novel coronavirus 2019(nCoV-2019) in Japan. Jpn. J. Infect. Dis. *73*, 304–307.
38. Nagata, N., Iwata-Yoshikawa, N., Sano, K., Ainai, A., Shiwa, N., Shirakura, M., Kishida, N., Arita, T., Suzuki, Y., Harada, T., et al. (2021). The peripheral T cell population is associated with pneumonia severity in cynomolgus monkeys experimentally infected with severe acute respiratory syndrome coronavirus 2. bioRxiv. https://www.biorxiv.org/content/10.1101/2021.01.07.425698v1.
39. Moriyama, S., Adachi, Y., Sato, T., Tonouchi, K., Sun, L., Fukushi, S., Yamada, S., Kinoshita, H., Nojima, K., Kanno, T., et al. (2021). Temporal maturation of neutralizing antibodies in COVID-19 convalescent individuals improves potency and breadth to circulating SARS-CoV-2 variants. Immunity *54*, 1841–1852.e4.

STAR★METHODS

KEY RESOURCES TABLE

REAGENT or RESOURCE	SOURCE	IDENTIFIER
Antibodies		
Human CD4 (clone M-T477) FITC	BD	Cat# 556615; RRID: AB_396487
Human CD8 (clone SK1) PerCP	BD	Cat# 347314; RRID: AB_400280
Human CD3 (clone SP34-2) APCCy7	BD	Cat# 557757; RRID: AB_396863
Human IFN-g (clone 4S.B3) PE	Biolegend	Cat# 502510; RRID: AB_315235
LIVE/DEAD Fixable Aqua Dead Cell Stain Kit	Invitrogen	Cat# L34957
HRP-conjugated anti-monkey IgG	Bethyl Laboratories	Cat# A140-102P; RRID: AB_67118
Bacterial and virus strains		
SARS-CoV-2 (strain wk-521)	Matsuyama et al., 2020	GenBank Accession # LC522975
F-deleted Sendai virus expressing N, M, and E (SeV-NME)	This manuscript	N/A
Biological samples		
Blood, swab, and tissue samples from cynomolgus macaques	This manuscript	N/A
Chemicals, peptides, and recombinant proteins		
Dulbecco's modified Eagle's medium (DMEM)	GIBCO	Cat# 11965-118
Phosphate Buffered Salts (PBS)	GIBCO	Cat# 10010-049
Penicillin/Streptomycin	GIBCO	Cat# 15140122
Fetal bovine serum	Cytiva	Cat# SH30396.03
Ficoll-Paque PLUS	Cytiva	Cat# 17144002
GolgiStop (monensin)	BD	Cat# 554724
Tween-20	SIGMA	Cat# P1379
Bovine serum albumin (BSA)	SIGMA	Cat# A8412
TMB substrate solution	Thermo Fisher Scientific	Cat# 34028
Overlapping peptides spanning the SARS-CoV-2 N	JPT Peptide Technologies	Cat# PM-WCPV-NCAP-1
Overlapping peptides spanning the SARS-CoV-2 M		Cat# PM-WCPV-VME-1
Overlapping peptides spanning the SARS-CoV-2 E		Cat# PM-WCPV-VEMP-1
recombinant SARS-CoV-2 M protein	RayBiotech	Cat# 230-01124
recombinant SARS-CoV-2 E protein	AcroBiosystems	Cat# ENN-C5128
Critical commercial assays		
QIAamp Viral RNA Minikit	QIAGEN	Cat# 52906
QuantiTect Probe RT-PCR Kit	QIAGEN	Cat# 204443
CytofixCytoperm kit	BD	Cat# 554714
TRIzol Plus RNA Purification Kit	Thermo Fisher Scientific	Cat# 12183555
Expi293 expression system	Thermo Fisher Scientific	Cat# A29133
TALON resin affinity chromatography	Clontech	Cat# 635503
Experimental models: Cell lines		
African green monkey (*Chlorocebus sabaeus*): Vero, VeroE6/TMPRSS2 cells	Matsuyama et al., 2020	N/A
Autologous herpesvirus papio-immortalized B-lymphoblastoid cell lines (B-LCLs)	This manuscript	N/A
Expi293F	Thermo Fisher Scientific	Cat# A14527

(*Continued on next page*)

Continued

REAGENT or RESOURCE	SOURCE	IDENTIFIER
Experimental models: Organisms/strains		
Macaca fascicularis (cynomolgus macaque)	Hamri Co., Ltd.	N/A
Oligonucleotides		
SARS2-LeaderF60: CGATCTCTT GTAGATCTGTTCTCT	Nagata et al., 2021 Nomura et al., 2021	N/A
SARS2-N28354R: TCTGAGGGT CCACCAAACGT		
SARS2-N28313Fam: TCAGCGAAAT GCACCCCGCA		
Recombinant DNA		
Plasmid: pcDNA-N	This manuscript	N/A
Plasmid: pcDNA-M	This manuscript	N/A
Plasmid: pcDNA-E	This manuscript	N/A
Software and algorithms		
GraphPad Prism v8	Graphpad	https://www.graphpad.com/scientific-software/prism/
FlowJo v9.2	FlowJo LLC	https://www.flowjo.com
FACS Diva v8.0.1	BD	http://www.bdbiosciences.com/instruments/software/facsdiva/index.jsp
Other		
96-well high-binding, half-area plates	Corning	Cat# 3690

RESOURCE AVAILABILITY

Lead contact

Requests for additional information and resources should be directed to the lead contact, Tetsuro Matano (tmatano@nih.go.jp).

Materials availability

All resources generated in this study are available from the lead contact upon request with a completed Materials Transfer Agreement.

Data and code availability

All data supporting the conclusion in this study are included in the main text and figures with supplemental information, and additional information will be available from the lead contact upon request.

EXPERIMENTAL MODEL AND SUBJECT DETAILS

Animals

Animal experiments using cynomolgus macaques (*Macaca fascicularis*, 3-7 years old) were performed at the National Institute of Infectious Diseases (NIID) after approval by the Committee on the Ethics of Animal Experiments in NIID (permission number: 520001) under the guidelines for animal experiments in accordance with the Guidelines for Proper Conduct of Animal Experiments established by the Science Council of Japan (http://www.scj.go.jp/ja/info/kohyo/pdf/kohyo-20-k16-2e.pdf). Gender and age of animals used in this study are described in Table S1. Blood and nasopharyngeal swab collection, vaccination, and virus inoculation were performed under ketamine anesthesia. Macaques were euthanized by whole blood collection under deep anesthesia and subjected to necropsy on day 7 or 9 post-infection.

Cell lines

Vero and VeroE6/TMPRSS2 cells (Matsuyama et al., 2020) were maintained in Dulbecco's modified Eagle's medium (DMEM, GIBCO) supplemented with 10% heat-inactivated fetal bovine serum (Cytiva) and 50 U/mL penicillin/streptomycin (Thermo Fisher Scientific) at 37°C supplied with 5% CO2. Expi293F cells (Thermo Fisher Scientific) were maintained in Expi293 expression medium (Thermo Fisher Scientific).

METHOD DETAILS

Animal experiments

For vaccination, we constructed pcDNA-N, pcDNA-M, and pcDNA-E plasmid DNAs by introducing cDNAs encoding nucleocapsid (N), membrane (M), and envelope (E) proteins of the SARS-CoV-2 wk-521 strain (2019-nCoV/Japan/TY/WK-521/2020, GenBank Accession LC522975), respectively, into pcDNA3.1 (Invitrogen). We also constructed a replication-incompetent F-deleted Sendai virus (SeV) vector[30,35] expressing N, M, and E (SeV-NME). We used two vaccine protocols in this study (Table S1). The first group of three cynomolgus macaques (V11, V12, and V13) received intramuscular vaccination with pcDNA-N (4 mg), pcDNA-M (2 mg), and pcDNA-E (2 mg) twice on days 0 and 4 and intranasal vaccination with SeV-NME (5×10^9 cell infectious unit [CIU]) at week 5 after the first vaccination. The second group of four cynomolgus macaques (V14, V15, V16, and V17) received intranasal SeV-NME vaccination twice with a 5-week interval.

SARS-CoV-2 wk-521 was expanded in Vero E6/TMPRSS2 cells[32] and harvested to prepare a virus challenge stock. Virus infectivity was assessed by detection of cytopathic effect (CPE) on Vero E6/TMPRSS2 cells and determination of endpoint titers. Virus challenge experiments 1 and 2 were performed separately because of the limitation of cage numbers in the facility. All of the challenge experiments were performed using the same SARS-CoV-2 stock. Vaccinated cynomolgus macaques were intranasally challenged with 10^5 (exactly 7.5×10^4) $TCID_{50}$ of SARS-CoV-2 at week 6 after the last vaccination. Four unvaccinated cynomolgus macaques (N031, N032, N041, and N042) were also intranasally challenged with 10^5 $TCID_{50}$ of SARS-CoV-2. Macaques were euthanized and subjected to necropsy on day 7 (V12, V14, V15, V17, N032, and N041) or 9 (V11, V13, V16, N031, and N042) post-infection. Data on additional five cynomolgus macaques (N012, N013, N022, D024, and D025) intranasally infected with 10^5 $TCID_{50}$ of the same SARS-CoV-2 stock in our previous study[23] were used as historical unvaccinated controls (Table S1).

Analysis of antigen-specific T-cell responses

Viral antigen-specific T-cell frequencies were measured by flow cytometric analysis of interferon-γ (IFN-γ) induction after specific stimulation as described previously.[23,36] PBMCs were prepared from whole blood by density gradient centrifugation using Ficoll-Paque PLUS (Cytiva). Lymph node-derived lymphocytes were prepared from minced lymph nodes by density gradient centrifugation using Ficoll-Paque PLUS. For analysis of SARS-CoV-2 N-, M-, and E-specific T-cell responses, autologous herpesvirus papio-immortalized B-lymphoblastoid cell lines (B-LCLs) were pulsed with peptide pools (at a final concentration of more than 0.1 μM for each peptide) using panels of overlapping peptides spanning the SARS-CoV-2 N, M, and E amino acid sequences (PM-WCPV-NCAP-1, PM-WCPV-VME-1, and PM-WCPV-VEMP-1; JPT Peptide Technologies). For analysis of SeV-specific T-cell responses, autologous B-LCLs were infected with SeV. PBMCs or lymph node-derived lymphocytes were cocultured with these B-LCLs in the presence of GolgiStop (monensin, BD) for 6 hours. Intracellular IFN-γ staining was performed using a CytofixCytoperm kit (BD) with LIVE/DEAD Fixable Aqua Dead Cell Stain Kit (Invitrogen), anti-CD3 APC-Cy7 (SP34-2; BD), anti-CD4 FITC (M-T477; BD), anti-CD8 PerCP (SK1; BD), and anti-IFN-γ PE (4S.B3; BioLegend). Stained cells were analyzed by BD FACS Canto II with FACS Diva v8.0.1 (BD) and FlowJo v9.2 (FlowJo LLC). Specific T-cell frequencies were calculated by subtracting nonspecific IFN-γ^+ T-cell frequencies from those after peptide-specific stimulation. Specific T-cell frequencies more than 0.02% of $CD4^+$ or $CD8^+$ T cells were considered positive.

Detection of SARS-CoV-2 RNAs

Swab RNAs were extracted from 0.2 ml of swab solutions (1ml of DMEM with 2% fetal bovine serum [Cytiva]) using QIAamp Viral RNA Minikit (QIAGEN) and subjected to real-time RT-PCR for viral RNA quantitation[37] using QuantiTect Probe RT-PCR Kit (Qiagen) and QuantStudio 5 (Thermo Fisher Scientific). Swab RNAs were also subjected to real-time RT-PCR for measurement of viral subgenomic RNA (sgRNA) levels[38] using the following primers: SARS2-LeaderF60 (5'-CGATCTCTTGTAGATCTGTTCTCT-3'), SARS2-N28354R (5'-TCTGAGGGTCCACCAAACGT-3'), and SARS2-N28313Fam (FAM-TCAGCGAAATGCACCCCGCA-TAMRA). Viral RNA or sgRNA levels less than 3×10^3 copies/swab were undetectable. Tissue RNAs were extracted from homogenized tissues by using TRIzol Plus RNA Purification Kit (Thermo Fisher Scientific) with phenol-chloroform extraction and subjected to real-time RT-PCR for detection of viral RNAs.

Virus recovery from swabs

Vero E6/TMPRSS2 cells in 96-well plates were added with 10-fold serially diluted swab solutions and cultured for 4 days without medium change. Virus recovery was assessed by detection of CPE and determination of endpoint titers. Swab samples with virus titers greater than 1×10^2 $TCID_{50}$/swab were considered positive.

Analysis of SARS-CoV-2-specific NAb responses

Endpoint plasma titers for inhibiting 20 $TCID_{50}$ of SARS-CoV-2 infection on Vero cells were measured as described previously.[23,39] Plasma samples were heat inactivated for 30 min at 56°C. Serial two-fold dilutions of heat-inactivated plasma were tested in quadruplicate. In each mixture for quadruplicate testing, 40 μl of diluted plasma were incubated with 40 μl of 80 $TCID_{50}$ SARS-CoV-2 wk-521. After incubation for 45 min at room temperature, 20 μl of the mixture was added to each of four wells (1×10^4 Vero cells/well) in a 96-well plate. Three days later, virus infectivity was assessed by detection of CPE to determine the endpoint titers. The lower limit of detection was 1:10.

Analysis of SARS-CoV-2 N-, M-, and E-specific binding antibody responses

For preparation of a recombinant N antigen, the synthesized human codon-optimized nucleotide sequence encoding the N protein of the SARS-CoV-2 (GenBank Accession MN994467) was obtained from Eurofins Genomics. The cDNA encoding N protein (amino acids 1-419) along with the signal peptide (amino acids 1-24; MPMGSLQPLATLYLLGMLVASCLG), a histidine-tag (HHHHHHHHH), and an avi-tag (GLNDIFEAQKIEWHE) was cloned into a CMV promoter-driven expression plasmid, and the plasmid was transfected into Expi293F cells (Thermo Fisher Scientific). The culture supernatant was harvested on day 5 post-transfection and subjected to purification of the recombinant N protein using a TALON resin affinity chromatography (Clontech). SARS-CoV-2 N-, M-, and E-specific binding antibody responses in plasma were measured by ELISA using the recombinant N protein described above, a recombinant SARS-CoV-2 M protein (RayBiotech), and a recombinant SARS-CoV-2 E protein (AcroBiosystems). The 96-well high-binding, half-area plates (Corning) were coated with the recombinant proteins (N: 1 μg/ml; M: 1 μg/ml; E: 0.2 μg/ml) at 4°C overnight. The plates were washed in PBS containing 0.05% Tween-20 and blocked with PBS containing 3% bovine serum albumin (BSA; Sigma) at 37°C for 1 hour. The antigen-coated plates were incubated with plasma diluted by 100 for N, 500 for M, and 1,000 for E, respectively, at 37°C for 1 hour. Antibodies bound to antigens were detected by OD_{450} after treatment with horseradish peroxidase (HRP)-conjugated anti-monkey IgG (Bethyl Laboratories) followed by TMB substrate solution (Thermo Fisher Scientific). A cut-off value was determined by the "Mean + 3 × SD" value, where Mean is the mean and SD is the standard deviation of negative control (without plasma) samples.

Histopathological analysis of the lung tissue obtained at necropsy

Hematoxylin and eosin (H&E)-stained samples were obtained from individual lobes (right upper, middle, lower, and accessory lobes and left upper [upper-middle], middle, and lower lobes). The number of lobes exhibiting lesions (epithelial degeneration with cell debris, slight peri-bronchial inflammatory cell infiltration, macrophage accumulation with alveolar wall thickening, interstitial infiltration of neutrophils, eosinophils, or mononuclear cells with airspace macrophages, and/or lymphoid cell aggregation in bronchial associated lymphoid tissue [BALT] or around blood vessels) was counted (Figure S4). No severe bronchiolitis or intestinal pulmonary inflammation was observed.

QUANTIFICATION AND STATISTICAL ANALYSIS

Statistical analyses were performed using Prism software (GraphPad Software, Inc.) with significance set at p values of <0.05. Comparisons were performed by Mann-Whitney U test. Correlation analyses were performed by Spearman's test.